Journal of Inflammation Research

Dovepress
Taylor & Francis Group

Open Access Full Text Article

ORIGINAL RESEARCH

Rbms3 Upregulation in Mesenchymal Stem Cells Impairs Fracture Healing in Type 2 Diabetes Mellitus

Changjiang Liu[1,2,*], Yifeng Yu[3,*], Liang Tian[1,2], Yuting Liu[1,2], Dong Zhang[1,2], Aixi Yu[1,2]

[1]Department of Orthopedics, Zhongnan Hospital of Wuhan University, Wuhan, Hubei, 430071, People's Republic of China; [2]Hubei Clinical Medical Research Center of Trauma and Microsurgery, Wuhan, Hubei, 430071, People's Republic of China; [3]Department of Orthopedics, Renmin Hospital, Wuhan University, Wuhan, Hubei, 430071, People's Republic of China

*These authors contributed equally to this work

Correspondence: Dong Zhang; Aixi Yu, Department of Orthopedics, Zhongnan Hospital of Wuhan University, Wuhan, Hubei, 430071, People's Republic of China, Email zhangdongemail@whu.edu.cn; yuaixi@whu.edu.cn

Background: Fracture healing can be delayed or impaired in individuals with abnormal conditions, including Type 2 Diabetes Mellitus (T2DM). Mesenchymal stem cells (MSCs) are critical to the process of fracture healing and are found to be impaired in T2DM. Although some research has been conducted to address this, the specific mechanisms remain poorly understood and warrant further exploration.

Methods: We downloaded transcriptomic and single-cell RNA sequencing (scRNA-seq) data, performed multiple analyses (differential expression, ssGSEA, co-expression, GO, KEGG, GSEA, and cell clustering identification), and utilized tools (GeneMINIA and Metascape) to investigate alterations in MSCs under diabetic condition. Further validation and exploration were carried out through in vitro experiments (cell transduction, flow cytometry, ALP staining, ARS, qPCR, and Western blotting) and in vivo experiments (micro-CT, histological staining, and immunohistochemistry).

Results: Our study identified differentially expressed genes from fracture healing and non-union cases in human samples, suggesting abnormal immune infiltration and disrupted biological processes. ScRNA-seq analysis further revealed significant alterations in MSCs under diabetic conditions with enriched pathways, including MAPK, TGF-β, and P53 signaling pathways. Integrating with transcriptomic analysis, we identified *Rbms3*, which was significantly upregulated in diabetic MSCs and further validated in bone samples from patients at our institution. The upregulation of *Rbms3* impaired fracture healing by modulating the MAPK signaling pathway, leading to reduced MSC osteogenic differentiation *in vitro* and impaired bone regeneration in vivo.

Conclusion: The upregulation of *Rbms3* in MSCs under diabetic conditions contributes to impaired fracture healing by modulating the MAPK signaling pathway.

Keywords: bioinformatics, single-cell RNA-sequencing analysis, T2DM, fracture non-union, bone healing

Introduction

Fractures are among the most prevalent musculoskeletal disorders worldwide, primarily resulting from trauma, inflammation, and pathological conditions such as osteoporosis and diabetes.[1–3] Epidemiological studies highlight their universal occurrence and indicate that nearly everyone is likely to experience a fracture in developing countries. While most fractures can heal with appropriate medical intervention, approximately 5–10% of fracture patients experience delayed healing or non-union, which not only prolongs patient suffering but also increases the burden on healthcare systems.[4] Consequently, extensive efforts have been dedicated to improving the fracture healing process, however, the intricate and multifactorial nature of fracture healing remains a significant obstacle.[5]

Mesenchymal stem cells (MSCs) are the key cells of bone regeneration and play a central role in the biological process of fracture healing.[6–8] They migrate to the fracture site, proliferate to expand the local cell pool and differentiate

Received: 16 January 2025
Accepted: 5 July 2025
Published: 21 July 2025

into osteoblasts, which are directly responsible for bone formation. Numerous studies have highlighted the potential of MSCs to improve bone healing. For instance, Lin et al demonstrated that enhancing the homing ability of MSCs can accelerate bone healing.[9] Guo et al showed that regulating collagen degradation promotes MSC migration and increases new bone formation.[10] However, further research is necessary to explore the relationship between delayed bone healing and various diseases.[11] Among these conditions, Type 2 Diabetes Mellitus (T2DM) stands out as a significant factor, as it is closely associated with both the incidence and impaired healing of fractures.[12] Moreover, the prevalence of T2DM continues to rise annually, making it an increasingly important issue in bone healing research. Studies have shown that in the diabetic environment, MSCs exhibit impaired functionality, including a shift from osteoblastic to adipocytic differentiation and alterations in cellular properties and molecular mechanisms.[13,14] However, the specific impact of T2DM on MCSs during the fracture healing process remains inadequately explored.

Recent advances in genomic sequencing technologies, especially single-cell RNA (scRNA) sequencing, have revolutionized disease mechanism research.[15] ScRNA sequencing enables detailed analysis of gene expression at the individual cell level, However, studies integrating single-cell analysis technologies to explore the effects of diabetes on fracture healing remain limited. In this study, we employed transcriptomic and single-cell sequencing analyses to uncover the functional alterations of MSCs under diabetic conditions. We found that the *Rbms3* gene was significantly upregulated in the diabetic and non-union environment, and it inhibited fracture healing by modulating the MAPK signaling pathway. The *Rbms3* gene encodes an RNA-binding protein that regulates post-transcriptional gene expression by binding to single-stranded RNA.[16] Previous studies have reported that *Rbms3* participates in various biological processes, such as embryogenesis, liver fibrosis, tumor progression, and jaw necrosis.[17] Overall, our findings provide insights into the mechanisms underlying diabetic non-union fractures and offer valuable perspectives for the development of future therapeutic strategies.

Materials and Methods

Ethical Statement

All animal experiments were conducted in accordance with the guidelines for laboratory animals established by the Wuhan University Center and Use of Laboratory Animals and were approved by the Experimental Animal Welfare Ethics Committee of Zhongnan Hospital, Wuhan University (Approval Number: WP2020-08023). The human studies were reviewed and approved by the Medical Ethics Committee for Clinical Research at Zhongnan Hospital (Approval Number: 20210007). Written informed consent was obtained from all participants involved in the study.

Data Collection, Processing, and Identification of Differentially Expressed Genes

In this study, we downloaded a dataset (GSE494) in the Gene Expression Omnibus (GEO) database, which included three matrix sets annotated by GPL92, GPL93, and GPL8300. The dataset contained six normal healing bone samples and six non-union bone samples in fracture patients. Data quality control, processing, and statistical analysis were performed using the "limma" R package. To eliminate batch effects, the "sav" R package was applied. Principal component analysis (PCA) was conducted using the "ggbiplot" R package. Differentially expressed genes (DEGs) were identified based on the criteria: $|\mathrm{Log_2(FoldChange)}| > 0.5$ and adjusted $P < 0.05$. The "pheatmap" and "ggplot2" R packages were used to generate heatmaps and volcano plots of the DEGs, respectively.

ssGSEA, Correlation, and Functional Enrichment Analyses

Single-sample Gene Set Enrichment Analysis (ssGSEA) is an extension of the Gene Set Enrichment Analysis (GSEA) method, allowing for the calculation of immune cell infiltration in each sample. To explore the potential relationship between fracture non-union and immune response, immune cell infiltration was estimated using the CIBERSORT algorithm. ssGSEA was performed using the "GSVA" R package, and violin plots were generated to compare the two groups using the "vioplot" R package. Additionally, the GeneMANIA database was employed to perform co-expression analysis and construct a protein-protein interaction (PPI) network for the identified genes. Functional enrichment was further analyzed using the Metascape database.

Processing of Single-Cell RNA-Seq Data from Normal and T2DM Samples

We obtained publicly available single-cell RNA sequencing data from the GEO database (GSE221936),[18] which included two samples: one from normal bone tissue and the other from T2DM bone. Data preprocessing was conducted using the "Seurat" R package (v4.3.0.1), where metadata were integrated with the expression matrix to create an S4 object. Cells were retained based on the following criteria: detection of 300 to 7,000 genes per cell and less than 10% mitochondrial gene content. The "Harmony" algorithm was applied to harmonize batch effects between the two datasets, followed by normalization using the "LogNormalize" method. Variable genes were identified using the "vst" method, selecting the top 2,000 highly variable genes. To reduce dimensionality, PCA, t-distributed stochastic neighbor embedding (t-SNE), and uniform manifold approximation and projection (UMAP) were performed. Clusters were identified and annotated based on known marker genes. Violin and bar plots were generated using the "ggpubr" and "ggplot2" R packages. Subsets of data corresponding to specific cell populations were extracted and re-analyzed using the "Seurat" R package. To explore the signaling pathways involved, Kyoto Encyclopedia of Genes and Genomes (KEGG) pathway analysis and GSEA were conducted on DEGs between the normal and T2DM groups.

Cell Isolation, Culture, and Lentiviral Transduction

Bone marrow-derived MSCs were isolated from the femur and tibia of 6-week-old rats. After flushing the femoral bone marrow, the cells were maintained in α-MEM medium supplemented with 10% fetal bovine serum (FBS) and 1% penicillin/streptomycin. Cells were cultured in a humidified incubator at 37°C with 5% CO_2. After three passages, the cells were collected for flow cytometry analysis to detect specific cell markers. For cell transduction, Lenti-Rbms3 and Lenti-NC lentiviral vectors were purchased from GENERAL BIOL (Anhui, China). Transduction was performed when cells reached approximately 50% confluence. After 12 hours, the medium was replaced, and the cells were cultured for an additional 48 hours. Transduction efficiency was assessed by Western blotting.

Osteogenic Differentiation Assay

For the osteogenic differentiation assay, cells were cultured in α-MEM medium supplemented with 10% fetal bovine serum (FBS), 10 nM dexamethasone, 10 mM β-glycerophosphate, and 50 μM L-ascorbic acid. The medium was replaced with half-volume changes every 3 days. Osteogenic differentiation was evaluated on day 14 and day 21 using alkaline phosphatase (ALP) and alizarin red S (ARS) staining, respectively. To quantify ARS results, the stained cells were gently rinsed with deionized water and incubated with 100 mM cetylpyridinium chloride in 10 mM sodium phosphate buffer (pH= 7.0) at room temperature for 1 hour, and the absorbance at 562 nm was measured. The expression of osteogenic-related genes, including *Runx2, Opn, Spp1, Alp*, and *Bmp2*, was also assessed in both groups. Stained images were observed under a light microscope.

In vivo Bone Repair Experiment Evaluation

Twenty-four male Sprague-Dawley (SD) rats (6–8 weeks old) were used to evaluate femoral defect repair in vivo. Anesthesia was induced by intraperitoneal injection of 2% sodium pentobarbital. After shaving and disinfecting the surgical site, a longitudinal incision (~1.5 cm) was made on the distal femur. A 3 mm diameter drill was employed to create a unilateral bone defect under controlled conditions, ensuring that surrounding tissues were preserved and fractures were avoided. The surgical site was irrigated with sterile PBS, and the incision was closed in layers. Postoperatively, the rats received injections of Lenti-Rbms3 lentivirus (1×10^{10} virus particles/10 μL) twice a week at the defect site. The animals were euthanized at 4 weeks post-surgery for subsequent analysis. The repair of the femoral defect in rats was evaluated using a high-resolution micro-CT system (SkyScan 1176; Bruker micro-CT, Kontich, Belgium).

Histological Analysis

Following micro-CT scanning, the specimens were fixed in 4% paraformaldehyde at 4°C for 48 hours. For paraffin embedding, the specimens were decalcified in 0.5 M EDTA at 4°C, followed by serial sectioning into 8 μm thick slices, which were subjected to H&E, Masson's, and immunohistochemical staining.

Quantitative Polymerase Chain Reaction (qPCR) Examination

Total RNA was extracted using TRIzol reagent (Invitrogen), and its concentration was measured using a Nanodrop spectrophotometer (Thermo Fisher Scientific). cDNA synthesis was performed using the PrimeScript RT Master Mix (TaKaRa, Japan). Quantitative real-time PCR (qRT-PCR) was conducted with the PowerUp™ SYBR™ Green Master Mix (Thermo Fisher Scientific). The relative expression levels were calculated using the 2^−ΔΔCt method. Primer sequences were listed in Supplementary Table 1.

Western Blotting

Total protein was extracted from MSCs using a cell lysis buffer (Beyotime, Shanghai, China) and quantified using the BCA assay kit (Thermo Fisher Scientific). The soluble proteins were separated by 10% SDS-PAGE and transferred to PVDF membranes. After blocking with 5% skimmed milk, the membranes were incubated with specific primary antibodies (Supplementary Table 2). Following incubation with the secondary antibodies, chemiluminescence was employed for protein visualization.

Statistical Analysis

All experiments were performed in triplicate, and data are presented as mean ± SD. Statistical analysis was performed using Student's *t*-test or one-way ANOVA (GraphPad Prism 8), with statistical significance set at $P < 0.05$.

Results

Transcriptome Sequencing Reveals Genes and Pathways Associated with Delayed Bone Healing

We first downloaded and processed sequencing data from bone tissue samples of twelve individuals (Figure 1A). Since the data were obtained from a public database, ethical concerns were not applicable. Next, based on gene expression levels, we performed a PCA, which revealed a clear separation between the Non-union (red) and Normal (blue) groups along the PC1 and PC2 axes, accounting for 26.0% and 16.1% of the total variance, respectively. This distinct clustering indicated significant biological or molecular differences between the two groups, warranting further investigation into the underlying factors contributing to non-union (Figure 1B). The volcano plot (Figure 1C) illustrated the differential gene expression between the normal and non-union groups, identifying 16 upregulated and 20 downregulated genes. Notably, genes such as *RBMS3, CTSO*, and *MS4A1* were significantly upregulated in the non-union group (red), while genes like *SOCS3, CREM*, and *TNPO1* were significantly downregulated (green). The volcano plot for these genes was displayed in Figure 1D. In addition, a violin plot was used to compare immune cell infiltration between the normal and non-union groups. Significant differences were observed in the proportions of activated B cells ($P = 0.030$), activated dendritic cells ($P = 0.015$), and Type 1 T-helper cells ($P = 0.009$), suggesting that immune cell distribution may be associated with the non-union condition. Meanwhile, no significant differences were found in CD56+ natural killer cells ($P = 0.699$) or natural killer T cells ($P = 0.937$) (Figure 1E). A considerable proportion of co-expression relationships, particularly those related to osteoblast regulation, differentiation, and lymphocyte proliferation, were revealed in the GeneMINIA database (Figure 1F). Furthermore, Gene Ontology (GO) enrichment analysis using the Metascape database identified several significantly enriched biological processes (Figure 1G). The most enriched process was "cellular response to leukemia inhibitory factor" (GO:1990830), followed by "response to hypoxia" (GO:0001666) and "positive regulation of neuron death" (GO:1901216). These illustrated that non-union was associated with such biological processes, highlighting the role of inflammation, hypoxia, and cell death.

Analyses of Gene Expression Changes at the Single-Cell Level in a T2DM scRNA Sequencing Dataset

We further investigated the single-cell sequencing dataset. The UMAP plots illustrated the clustering of single-cell RNA sequencing data, clearly delineating distinct cell populations based on gene expression profiles. A total of 20 clusters were identified, each corresponding to specific cell types as shown in the right panel. Notably, key cell types such as

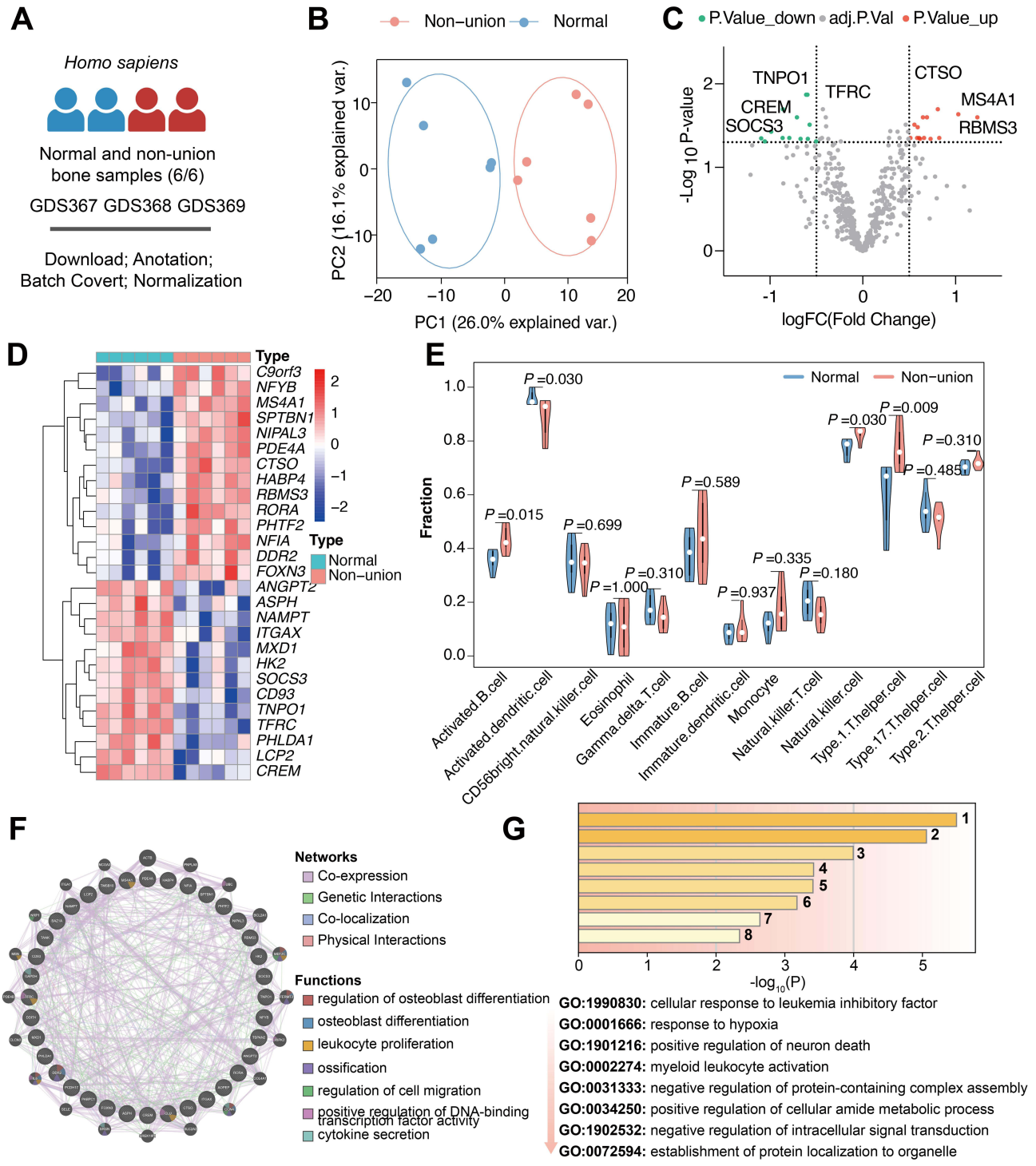

Figure 1 Transcriptomic and functional analysis of normal and non-union bone samples. (**A**) RNA-seq data from GEO datasets were downloaded and processed. (**B**) PCA analysis shows a clear separation between normal and non-union samples. (**C**) Volcano plot of differential expression analysis. (**D**) Heatmap of differential expression analysis. (**E**) Immune cell infiltration in two groups. (**F**) Co-expression network analysis uncovers functional clusters related to osteoblast differentiation in GeneMINIA database. (**G**) Functional enrichment analysis in the Metascape database.

osteoblasts, mesenchymal stem cells (MSCs), and erythroid cells were distinctly identified, with osteoblasts further categorized into subtypes (Osteoblast I–VI) (Figure 2A). Subsequently, we compared the proportions of various cell types between the T2DM and control groups (Figure 2B and C). The control group showed a higher abundance of mesenchymal cells (Mesenchymal cell I) and osteocytes. A significant reduction in pre-osteoblasts was observed in the

https://doi.org/10.2147/JIR.S517789

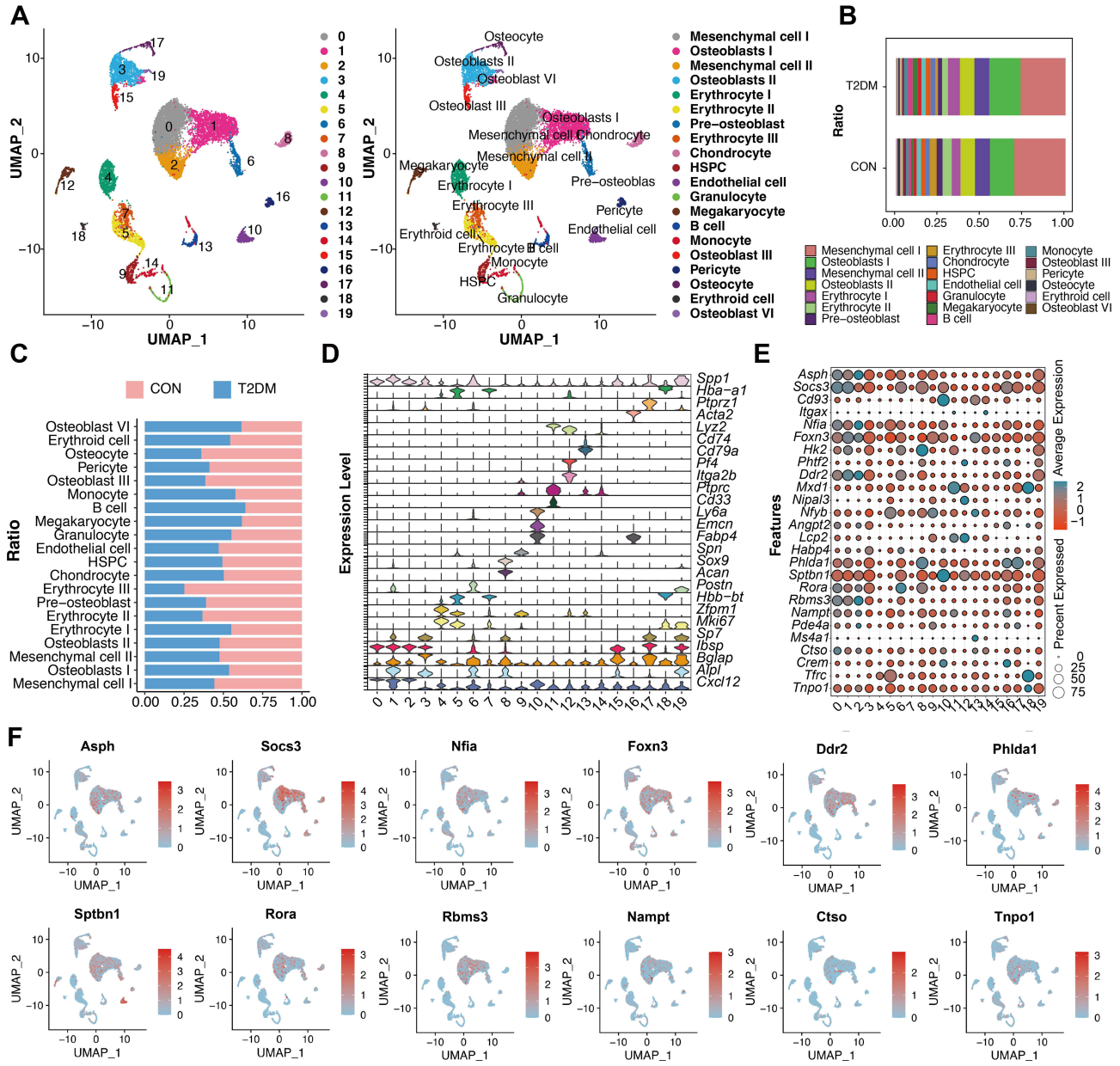

Figure 2 Single-cell transcriptomic profiling of bone tissue in normal and diabetic conditions and integrated them with transcriptomic analysis. (**A**) UMAP visualization of single-cell transcriptomic data showing 20 distinct cell clusters with annotations. (**B**) and (**C**) Comparison of cell type proportions between T2DM and control groups. (**D**) Violin plots displaying expression levels of representative specific marker genes across cell clusters. (**E**) Dot plot of DEGs from RNA-seq analysis across all cell clusters, with the size representing the percentage of cells expressing the gene and the color indicating average expression levels. (**F**) Feature plots illustrating UMAP-based spatial expression of selected DEGs.

T2DM group, suggesting that diabetes may disrupt the balance and differentiation potential within the bone marrow microenvironment, influencing the pathophysiology of bone metabolism under diabetic conditions. Cell type annotation was performed using the CellMarker tool and literature,[18,19] as demonstrated in Figure 2D.

Next, we explored the expression of DEGs from the transcriptomic data within the single-cell clusters (Figure 2E). The circle color denoted the average expression level of each gene, with blue indicating low expression and red indicating high expression. Circle size represented the percentage of cells within each cluster expressing the gene. For instance, *Socs3* and *Cd93* displayed high expression levels across multiple clusters, whereas genes like *Foxn3* and *Hk2* showed cluster-specific expression. The expression ratios and levels of *Rbms3, Ddr2*, and *Nampt genes* were relatively higher in clusters 0 and 2 than those in the other clusters, especially the *Rbms3* gene, representing correlations with the

specialized functions of MSCs. Finally, the top 12 genes expressed within these clusters were selected, and their expression patterns were visualized on the UMAP plots. Consistent with previous findings, the red areas in the UMAP plot of *Rbms3* were mainly distributed in MSCs, demonstrating relatively better specificity (Figure 2F).

Identification of scRNA Sequencing Subclusters

In the above scRNA sequencing analysis, we observed differences in the clustering of MSCs between the T2DM and control groups. The gene expression level alterations in MSCs under diabetic conditions may provide new insights into delayed bone healing associated with T2DM. Consequently, we performed further analysis on clusters 0 and 2. The t-SNE plot illustrated the distribution of various MSC subclusters in a low-dimensional space (Figure 3A). Five MSC subclusters were identified, including two adipogenic subpopulations (MSC-1 and MSC-2) and two osteogenic subpopulations (MSC-0 and MSC-3). Notably, MSC-4 exhibited transitional characteristics, potentially representing a state of adipogenic or osteogenic differentiation. The clustering within each subpopulation indicated their phenotypic similarities.[20] The top 10 differentially expressed genes in each cluster were presented in Figure 3B.

The *Rbms3* gene attracted our attention in both transcriptomic and scRNA analyses due to its significant differential expression between normal and non-healing groups in the transcriptome data analyses, as well as its high and specific expression in MSCs in scRNA sequencing results. Figure 3C illustrated the relationship between the re-annotated cell subclusters and the original UMAP plot cluster. Notably, *Rbms3* exhibited expression differences in clusters 0 and 3 within the re-annotated datasets. These clusters were associated with osteogenic MSCs, indicating a correlation between Rbms3 and osteogenic differentiation of MSCs. Furthermore, bar plots illustrated the elevated expression of *Rbms3* in clusters 0 and 3 ($P < 0.05$) (Figure 3D), consistent with the transcriptomic results. KEGG analysis revealed the pathways enriched in MSCs between diabetic and normal bone tissues (Figure 3E). The KEGG_MAPK_SIGNALING_PATHWAY showed a high enrichment score, suggesting its potential relevance. Figure 3F illustrated its enrichment in the GSEA analysis. To validate these findings, we collected bone tissue from diabetic delayed-healing patients and normal-healing patients at our institution. The qPCR results confirmed that *Rbms3* expression was significantly elevated in the T2DM and non-union group, especially in the patients with T2DM and non-union (Figure 3G).

Rbms3 Modulated Osteogenic Differentiation of MSCs

To further investigate the relationship between the *Rbms3* gene and osteogenic differentiation, we isolated primary bone marrow-derived MSCs. The morphology of the MSCs was shown in Figure 4A. Flow cytometry analysis indicated that these cells expressed CD73 and CD90 and almost did not express CD19 and HLA-DA (Figure 4B), confirming the successful isolation and culture of MSCs. Subsequently, *Rbms3* overexpression was verified by Western blotting in MSCs following Lenti-Rbms3 transduction (Figure 4C). ALP staining revealed that *Rbms3* overexpression led to reduced ALP activity on day 14, indicating its detrimental effect on early osteogenic differentiation of MSCs (Figure 4D). Similarly, ARS staining on day 21 showed a decrease in calcium deposition in the Lenti-Rbms3 group (Figure 4E and 4F). qPCR analyses further confirmed the expression levels of multiple osteogenesis-related genes, including *Opn, Ocn, Alp, Spp1*, and *Runx2* in the Lenti-Rbms3 groups were down-regulated, potentially explaining the alternation in osteogenic differentiation (Figure 4G).

Rbms3 Mediated Osteogenic Differentiation via MAPK Signaling Pathway

The aforementioned KEGG pathway analysis revealed that the MAPK signaling pathway was significantly enriched in MSC clusters, potentially suggesting its critical role in normal and diabetic bone healing. Previous studies have suggested that the MAPK signaling pathway is closely related to the osteogenic process.[21] As shown in Figure 5A, transduction of Lenti-Rbms3 inhibited the phosphorylation of ERK, JNK, and p38, indicating the involvement of the MAPK signaling pathway. To confirm its role, we cultured Lenti-Rbms3-transducted cells with or without a MAPK agonist (Cannabisin D, 50 μM). As shown in Figure 5B, the agonist significantly increased the phosphorylation levels of ERK1/2, p38, and JNK in Lenti-Rbms3-transducted cells, confirming the activation of the MAPK signaling pathway. In terms of osteogenic differentiation, ALP staining on day 14 showed increased ALP activity in the MAPK agonist-treated group, with higher calcium deposition observed on day 21, although still lower than in the Lenti-NC group (Figure 5C, Supplementary Figure 1). Furthermore, the protein expression of osteogenic

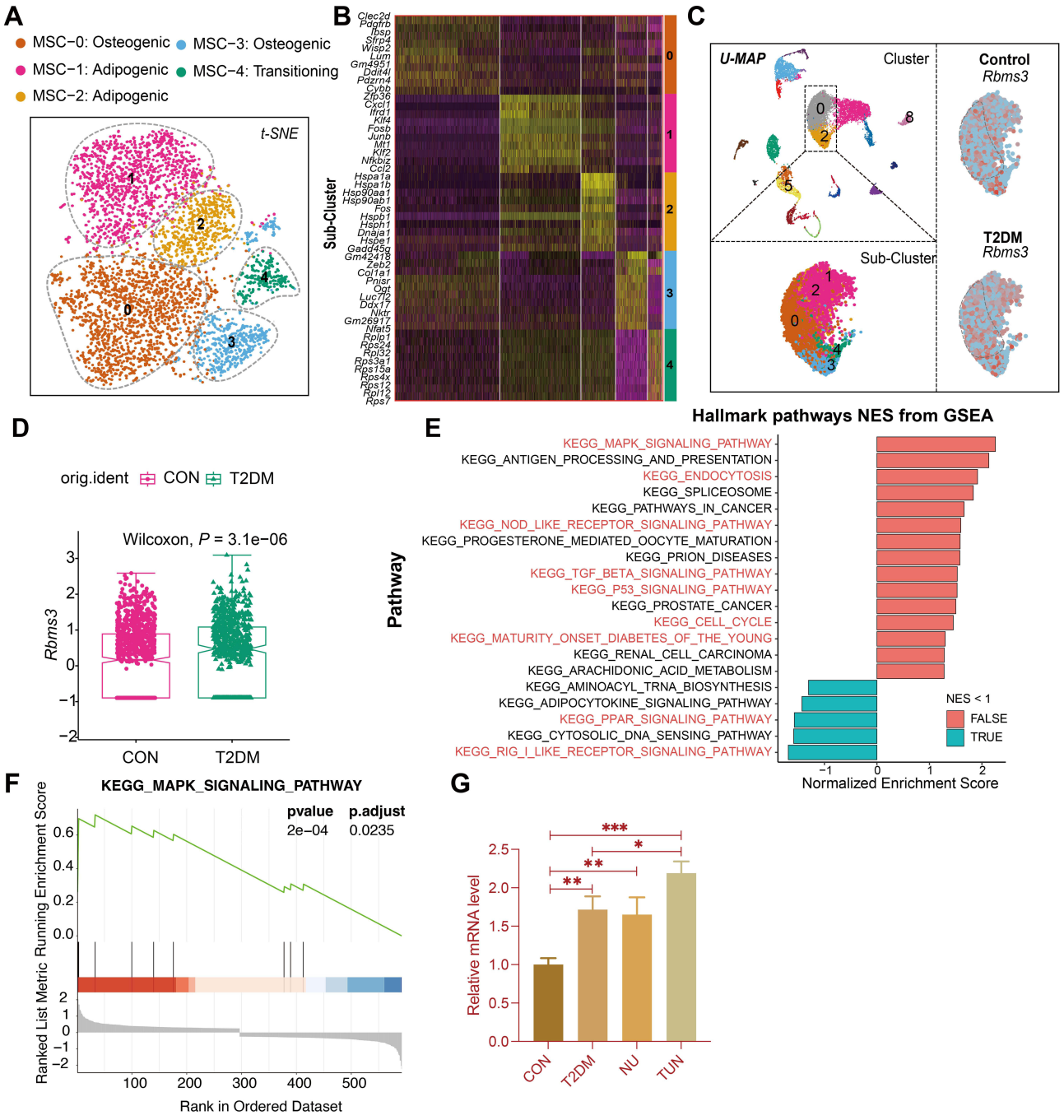

Figure 3 Sub-clustering analysis of mesenchymal stem cells (MSCs) and pathway enrichment in T2DM bone tissue. (**A**) t-SNE visualization of MSC sub-clusters, identifying osteogenic (MSC-0, MSC-3), adipogenic (MSC-1, MSC-2), and transitioning (MSC-4) states. (**B**) Heatmap showing distinct gene expression patterns among MSC sub-clusters. (**C**) UMAP analysis of MSC clusters and sub-clusters in control and T2DM groups. (**D**) Boxplot comparing Rbms3 expression between two groups. (**E**) GSEA analysis of hallmark pathways, highlighting significant associated enrichment pathways in red. (**F**) GSEA Enrichment plot for KEGG_MAPK_SIGNALING_PATHWAY. (**G**) qRT-PCR validation of RBMS3 expression in normal, T2DM, NU (non-union), and TUN (T2DM with non-union) bone tissues, (***p < 0.001, **p < 0.01, *p < 0.05).

markers such as BMP2, Col-1, RUNX2, and OSX was significantly upregulated following MAPK activation (Figure 5D). These findings suggested that *Rbms3* can mediate the MAPK signaling pathway and play a disadvantageous role in osteogenesis.

Overexpression of Rbms3 Delayed Bone Healing Process

Considering the inhibitory effects of the *Rbms*3 gene on the MAPK signaling pathway, we further investigated the role of *Rbms3* in bone healing in vivo to determine whether elevated expression of *Rbms3* can delay the healing process

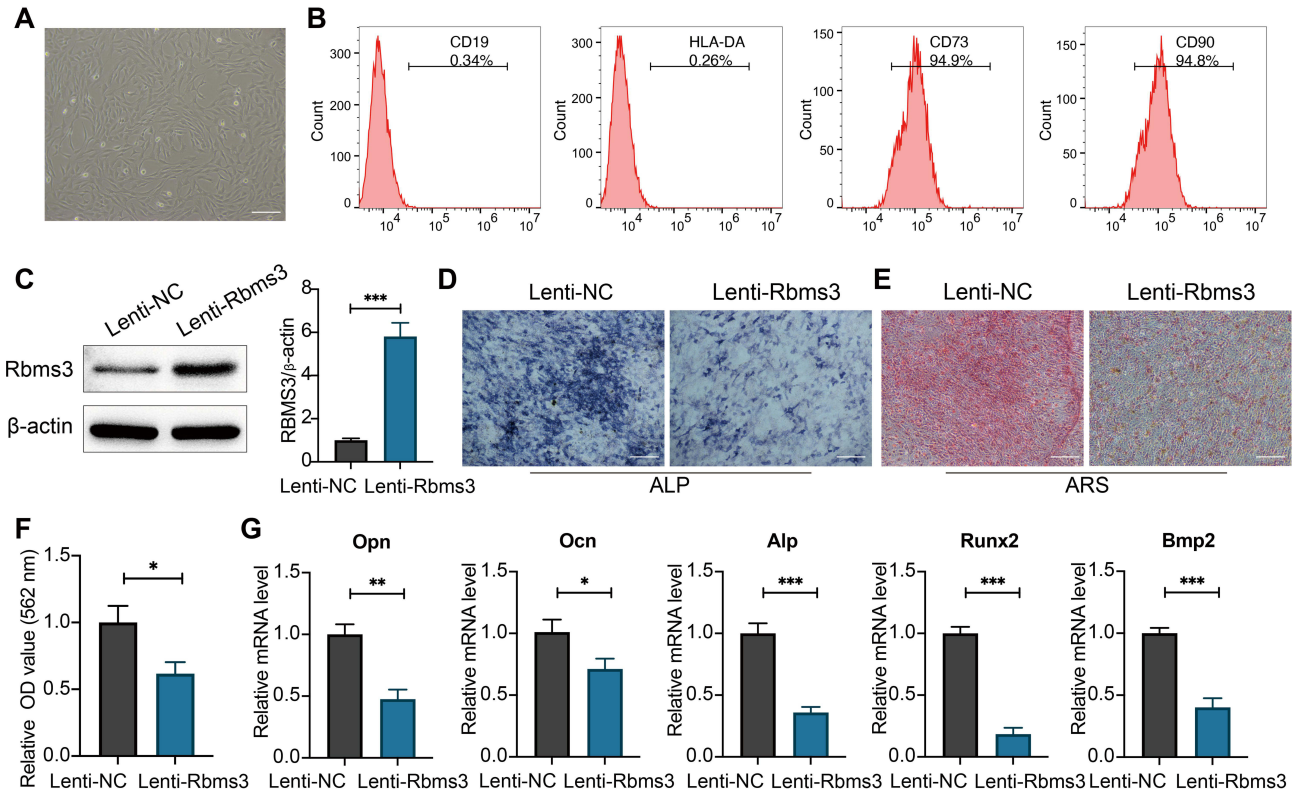

Figure 4 Overexpression of Rbms3 impaired osteogenic differentiation of MSCs. (**A**) Morphological observation of cultured mesenchymal stem cells (MSCs) under brightfield microscopy. Scale bars = 50 μm. (**B**) Flow cytometry analysis confirming MSC identity with positive expression of CD73 and CD90 and negative expression of CD19 and HLA-DR. (**C**) Western blot analysis showing significant upregulation of Rbms3 in MSCs transducted with Lenti-Rbms3. (**D**) Alkaline phosphatase (ALP) staining and (**E**) Alizarin Red staining showing reduced osteogenic differentiation in Lenti-Rbms3 MSCs. Scale bars = 100 μm. (**F**) Quantification of ARS staining showing a significant decrease in the Lenti-Rbms3 group. (**G**) qRT-PCR analysis of osteogenic markers (Opn, Ocn, Alp, Runx2, and Bmp2) revealing significantly reduced expression in the Lenti-Rbms3 group (*p < 0.05, **p < 0.01, ***p < 0.001).

(Figure 6A). Briefly, Lenti-NC, Lenti-Rbms3, and Lenti-Rbms3+ agonist were injected into the distal femoral defects of rats. The rats were sacrificed at 4 weeks, and their distal femurs were collected. CT results showed that compared to the Lenti-NC group, the Lenti-Rbms3 group exhibited larger bone defects, while treatment with the agonist appeared to be beneficial to defect healing (Figure 6B). Further quantitative analysis confirmed that the Lenti-Rbms3 group displayed less new bone formation (Figure 6C, Supplementary Figure 2). H&E staining analysis revealed no significant differences in inflammatory infiltration between the groups (Figure 6D). Masson's staining showed different collagen deposition patterns. Compared to Lenti-NC and Lenti-Rbms3+ agonist groups, the Lenti-Rbms3 group exhibited less collagen deposition, which was consistent with the CT image results. Similarly, immunohistochemistry staining for OCN indicated slightly lower levels of OCN in the bones of the Lenti-Rbms3 group (Figure 6E, 6F and 6G), which could explain the delayed healing observed.

Discussion

In the present study, we combined transcriptome sequencing and single-cell RNA sequencing (scRNA-seq) analyses to explore the functions of MSCs in bone non-union and T2DM. Our results revealed differences between MSCs from normal and diabetic bone tissues and identified that increased expression of the *Rbms3* gene in MSCs impaired the bone healing process, which involves the regulation of the MAPK signaling pathway. Alternating *Rbms3* expression or activating the MAPK signaling pathway could potentially benefit bone healing in diabetic patients.

Although extensive sequencing data have been provided in recent years, studies on non-tumor-related diseases remain limited, particularly in diabetic bone healing. ScRNA-seq data on diabetic bone healing are almost absent due to its high cost and strict tissue requirements. To address this, we integrated transcriptome data from patients with normal healing

https://doi.org/10.2147/JIR.S517789

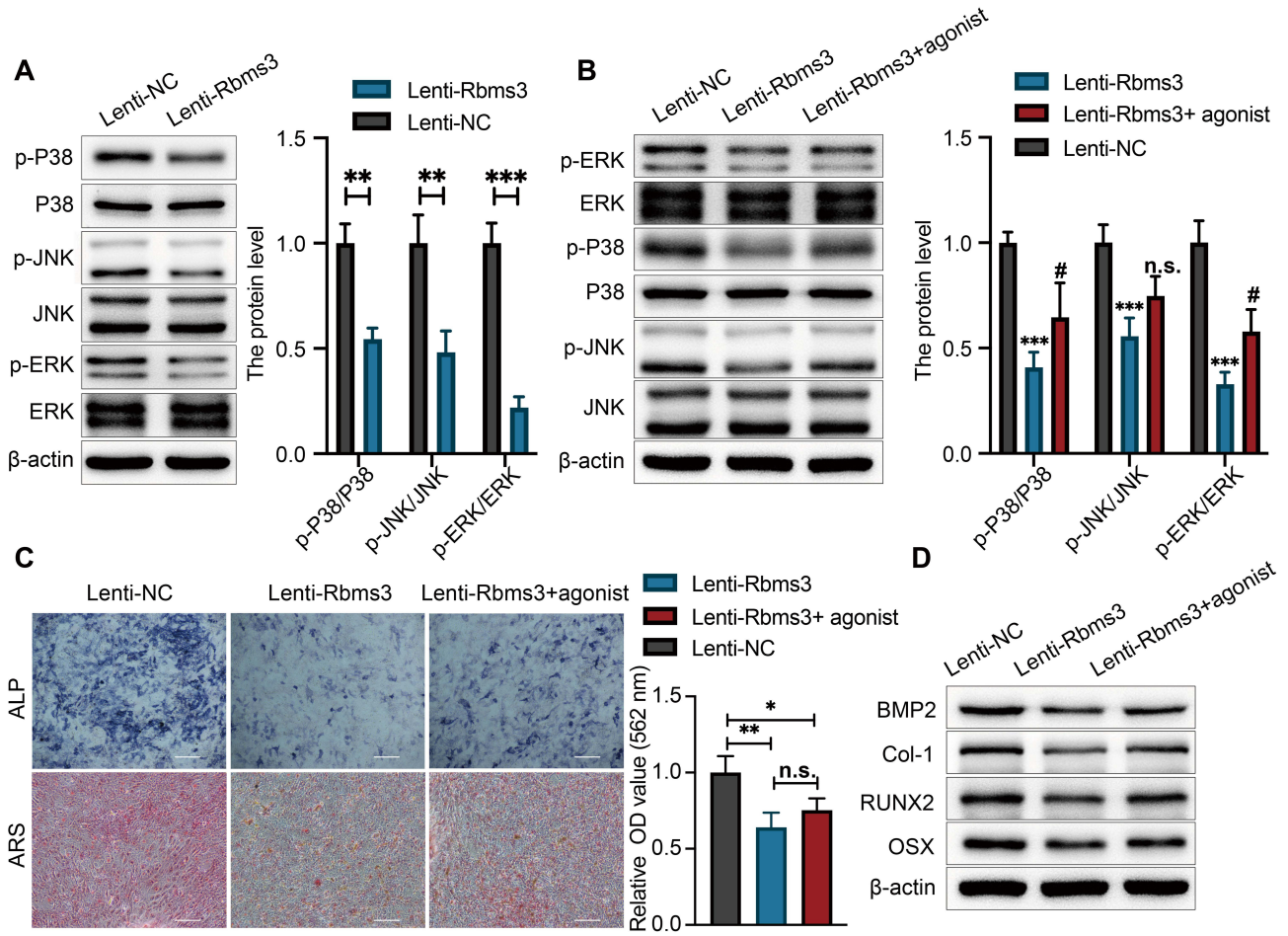

Figure 5 Rbms3 inhibited osteogenic differentiation of MSCs through suppression of MAPK signaling pathways. (**A**) Western blot analysis showing reduced phosphorylation levels of p38, JNK, and ERK in MSCs transducted with Lenti-Rbms3. (**B**) Rescue experiments with a MAPK agonist partially restored the phosphorylation levels of p38, JNK, and ERK in Lenti-Rbms3 MSCs (#, $p < 0.05$, Lenti-Rbms3 compared with Lenti-Rbms3+ agonist; n.s. = not significant). (**C**) ALP and Alizarin Red staining demonstrating decreased osteogenic differentiation in Lenti-Rbms3 MSCs, which was partially reversed by MAPK agonist treatment. (**D**) Western blot analysis showing expression of osteogenic markers (BMP2, COL-1, RUNX2, and OSX) in three groups. (*$p < 0.05$, **$p < 0.01$, ***$p < 0.001$). Scale bars = 100 μm.

and non-union and a scRNA-seq dataset. In transcriptomic analysis, we observed few DEGs between the non-union and normal groups, likely due to the sequencing process being conducted two decades ago and some gene alternations were overlooked. Nevertheless, the PCA and immune infiltration calculations revealed significant differences between the groups. Co-expression analysis of DEGs revealed processes related to bone development, including osteoblast differentiation. Functional enrichment analysis identified inflammation, hypoxia, and neuronal death as pathways potentially associated with non-union. In scRNA-seq analyses, a large number of cell clusters were identified, indicating different cellular states at various stages of bone biological processes. KEGG enrichment analysis of MSCs from diabetic and normal conditions highlighted several diabetes-related signaling pathways, shedding light on functional changes in MSCs under diabetic conditions. Notably, the *Rbms3* gene was significantly differentially expressed in transcriptome sequencing results and was widely expressed in MSCs, with differential expression observed between normal and diabetic MSCs. In subsequent experiments, we explored the effects of *Rbms3* on MSC function and bone healing process.

As to the *Rbms3* gene, a lot of research has focused on the oncogenic role of *Rbms3* in multiple cancers, including bladder, gastric, and prostate cancers. In non-tumor studies, *Rbms3* knockout in zebrafish leads to severe craniofacial defects, potentially due to its regulation influence on *Smad*1/2 stability, thus disrupting the TGF-β receptor pathway, emphasizing the essential role of the *Rbms3* gene.[22] However, the role of *Rbms3* in regulating normal cell proliferation appears to be tissue-specific. For instance, *Rbms3* can promote the proliferation of nucleus pulposus cells and inhibit matrix degradation through the Wnt/β-catenin pathway, thereby preventing intervertebral disc degeneration.[23] In contrast,

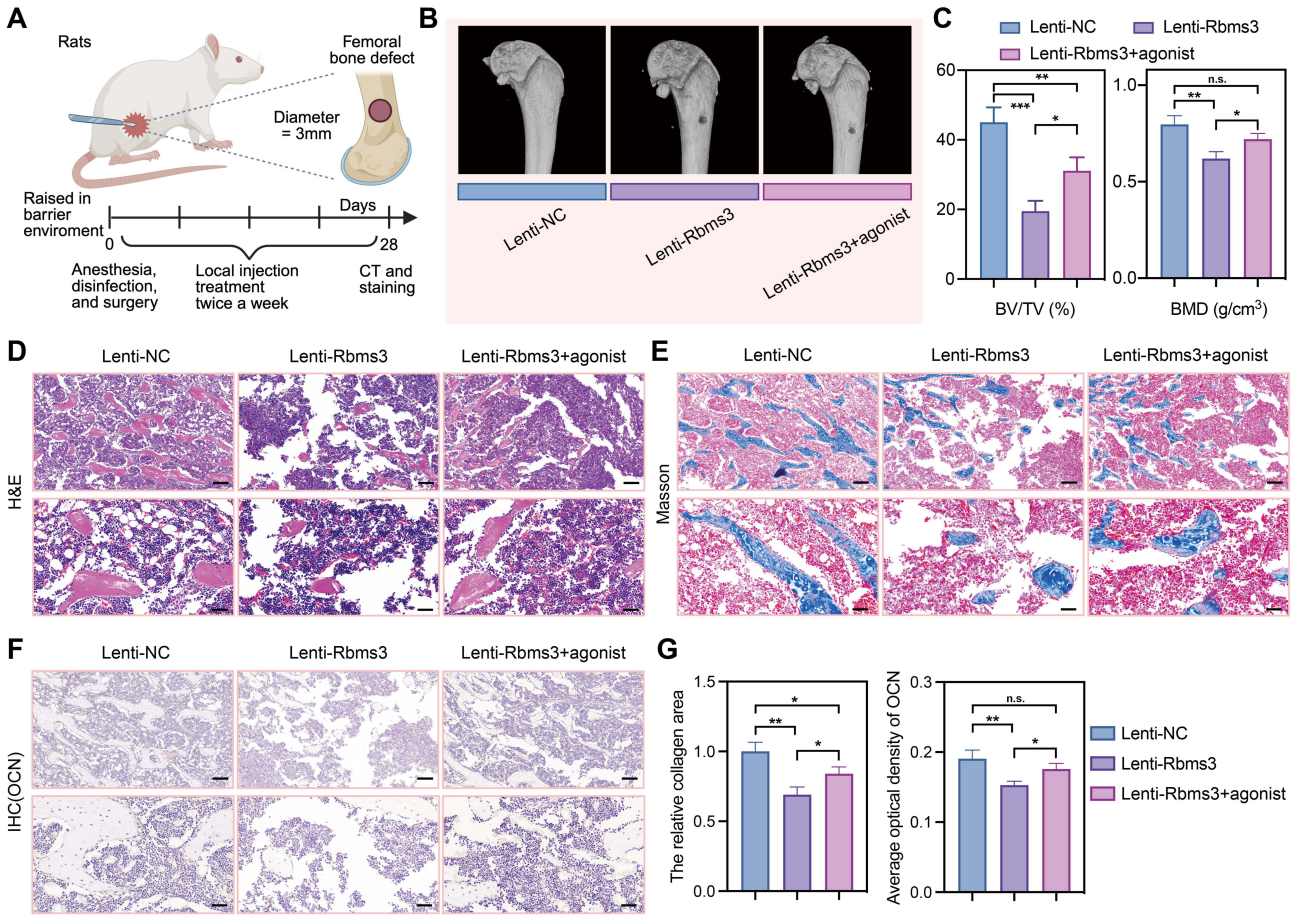

Figure 6 Rbms3 impaired bone regeneration in vivo through inhibition of osteogenic activity. (**A**) The schematic of the animal experiment. (**B**) and (**C**) Micro-CT images and quantitative analyses in the three groups. (**D**) H&E staining and (**E**) Masson's trichrome staining. (**F**) Immunohistochemical staining for OCN. Scale bars = 200 μm and 50μm, respectively. (**G**) Quantitative analyses of collagen area and OCN in the three groups. (*p < 0.05, **p < 0.01, ***p < 0.001).

the knockout of Rbms3 in chronic obstructive pulmonary disease (COPD) models can promote cell proliferation.[24] In bone-related research, statistical evidence suggests that elevated *Rbms3* expression negatively impacts bone density. Genome-wide association studies have shown that single nucleotide polymorphisms (SNPs) in the *Rbms3* gene may affect collagen expression, influencing bone tissue changes. Furthermore, *Rbms3* gene variants are associated with a 5.8-fold increased risk of bisphosphonate-related osteonecrosis of the jaw (BRONJ),[25] indicating the detrimental effects of *Rbms3* on bone health.

Similarly, the MAPK (Mitogen-Activated Protein Kinase) signaling pathway is a critical cellular signaling pathway involved in cell proliferation, differentiation, and apoptosis.[26] Numerous studies have demonstrated that the MAPK signaling pathway promotes osteoblast differentiation.[21,27,28] In bone repair research, activation of the MAPK signaling pathway has been shown to enhance osteoblast differentiation, thereby accelerating the bone healing process. However, research on the regulation of the MAPK signaling pathway by *Rbms3* remains scarce. In our study, we confirmed the inhibitory effect of *Rbms3* on the MAPK signaling pathway during osteogenic differentiation and bone healing processes in vitro and in vivo, providing a new insight into the diabetic bone healing process. Given its role in modulating bone healing, *Rbms3* could be a potential target for gene therapy or small molecules aimed at enhancing MSCs' function and promoting faster fracture healing. Future clinical studies could explore the feasibility of using Rbms3-based interventions, such as viral vector-mediated gene delivery or small molecules, to modulate its expression at fracture sites in diabetic patients. Meanwhile, clinical studies on the modulation of the MAPK signaling pathway have been extensively conducted, particularly in various cancer patients, such as those with lung cancer,[29] melanoma,[30] colorectal cancer,[31] and

https://doi.org/10.2147/JIR.S517789

thyroid cancer.[32] Pharmacological agents or molecular inhibitors that modulate MAPK signaling may provide a viable therapeutic strategy to improve bone repair.

However, there are some limitations to our study. First, the lack of single-cell sequencing data on diabetic bone healing still exists. Second, while we have demonstrated that *Rbms3* regulates the MAPK signaling pathway and osteoblast differentiation, further exploration of the specific regulatory mechanisms between them is necessary. Nonetheless, our combined analysis of scRNA-seq and human transcriptome data is worth learning. *Rbms3* expression level was validated in bone tissue samples from our institution and its function was investigated. More interesting research should focus on *Rbms3* genes and the diabetic bone healing process.

Ethical Statement

All animal experiments were conducted in accordance with the guidelines for laboratory animals established by the Wuhan University Center and Use of Laboratory Animals and were approved by the Experimental Animal Welfare Ethics Committee of Zhongnan Hospital, Wuhan University (Approval Number: WP2020-08023). The human studies were reviewed and approved by the Medical Ethics Committee for Clinical Research at Zhongnan Hospital (Approval Number: 20210007). Written informed consent was obtained from all participants involved in the study.

Acknowledgments

We would like to thank the public databases and study participants for voluntarily participating in this study.

Funding

This work was supported by grants from the National Natural Science Foundation of China (82072440), Zhongnan Hospital of Wuhan University, Excellent Doctor Fund Project (ZNYB2022015), Natural Science Foundation of Hubei Province (2024AFD167).

Disclosure

The authors declare that they have no competing interests.

References

1. Wildemann B, Ignatius A, Leung F, et al. Non-union bone fractures. *Nat Rev Dis Primers*. 2021;7(1):57. doi:10.1038/s41572-021-00289-8
2. Ruggiero C, Baroni M, Xenos D, et al. Dementia, osteoporosis and fragility fractures: intricate epidemiological relationships, plausible biological connections, and twisted clinical practices. *Ageing Res Rev*. 2024;93:102130. doi:10.1016/j.arr.2023.102130
3. Emanuelsson F, Afzal S, Jorgensen NR, Nordestgaard BG, Benn M. Hyperglycaemia, diabetes and risk of fragility fractures: observational and Mendelian randomisation studies. *Diabetologia*. 2024;67(2):301–311. doi:10.1007/s00125-023-06054-8
4. Einhorn TA, Gerstenfeld LC. Fracture healing: mechanisms and interventions. *Nat Rev Rheumatol*. 2015;11(1):45–54. doi:10.1038/nrrheum.2014.164
5. Menger MM, Laschke MW, Orth M, Pohlemann T, Menger MD, Histing T. Vascularization strategies in the prevention of nonunion formation. *Tissue Eng Part B Rev*. 2021;27(2):107–132. doi:10.1089/ten.teb.2020.0111
6. Lin H, Sohn J, Shen H, Langhans MT, Tuan RS. Bone marrow mesenchymal stem cells: aging and tissue engineering applications to enhance bone healing. *Biomaterials*. 2019;203:96–110. doi:10.1016/j.biomaterials.2018.06.026
7. Undale AH, Westendorf JJ, Yaszemski MJ, Khosla S. Mesenchymal stem cells for bone repair and metabolic bone diseases. *Mayo Clin Proc*. 2009;84(10):893–902. doi:10.4065/84.10.893
8. Pal D, Das P, Roy S, et al. Recent trends of stem cell therapies in the management of orthopedic surgical challenges. *Int J Surg*. 2024;110(10):6330–6344. doi:10.1097/JS9.0000000000001524
9. Lin W, Xu L, Zwingenberger S, Gibon E, Goodman SB, Li G. Mesenchymal stem cells homing to improve bone healing. *J Orthop Translat*. 2017;9:19–27. doi:10.1016/j.jot.2017.03.002
10. Guo Y, Ma S, Wang D, et al. HtrA3 paves the way for MSC migration and promotes osteogenesis. *Bioact Mater*. 2024;38:399–410. doi:10.1016/j.bioactmat.2024.05.016
11. Liu C, Liu Y, Yu Y, et al. Identification of up-regulated ANXA3 resulting in fracture non-union in patients with T2DM. *Front Endocrinol*. 2022;13:890941. doi:10.3389/fendo.2022.890941
12. Napoli N, Chandran M, Pierroz DD, et al. Diabetes working G: mechanisms of diabetes mellitus-induced bone fragility. *Nat Rev Endocrinol*. 2017;13(4):208–219. doi:10.1038/nrendo.2016.153
13. Cramer C, Freisinger E, Jones RK, et al. Izadpanah R: persistent high glucose concentrations alter the regenerative potential of mesenchymal stem cells. *Stem Cells Dev*. 2010;19(12):1875–1884. doi:10.1089/scd.2010.0009
14. Bueno NP, Kfouri CC, Copete IN, et al. Photobiomodulation treatments drive osteogenic versus adipocytic fate of bone marrow mesenchymal stem cells reversing the effects of hyperglycemia in diabetes. *Lasers Med Sci*. 2022;37(7):2845–2854. doi:10.1007/s10103-022-03553-9

15. Macosko EZ, Basu A, Satija R, et al. Highly parallel genome-wide expression profiling of individual cells using nanoliter droplets. *Cell*. 2015;161(5):1202–1214. doi:10.1016/j.cell.2015.05.002
16. Ruan X, Liu Y, Wang P, et al. RBMS3-induced circHECTD1 encoded a novel protein to suppress the vasculogenic mimicry formation in glioblastoma multiforme. *Cell Death Dis*. 2023;14(11):745. doi:10.1038/s41419-023-06269-y
17. Gornicki T, Lambrinow J, Mrozowska M, Podhorska-Okolow M, Dziegiel P, Grzegrzolka J. Role of RBMS3 novel potential regulator of the EMT phenomenon in physiological and pathological processes. *Int J Mol Sci*. 2022;23(18):10875. doi:10.3390/ijms231810875
18. Song F, Lee WD, Marmo T, et al. Osteoblast-intrinsic defect in glucose metabolism impairs bone formation in type II diabetic male mice. *Elife*. 2023;12:e85714.
19. Zhou Y, Yang D, Yang Q, et al. Single-cell RNA landscape of intratumoral heterogeneity and immunosuppressive microenvironment in advanced osteosarcoma. *Nat Commun*. 2020;11(1):6322. doi:10.1038/s41467-020-20059-6
20. Leimkuhler NB, Gleitz HFE, Ronghui L, et al. Heterogeneous bone-marrow stromal progenitors drive myelofibrosis via a druggable alarmin axis. *Cell Stem Cell*. 2021;28(4):637–652e638. doi:10.1016/j.stem.2020.11.004
21. Wang Z, Liu Q, Liu C, et al. Mg(2+) in beta-TCP/Mg-Zn composite enhances the differentiation of human bone marrow stromal cells into osteoblasts through MAPK-regulated Runx2/Osx. *J Cell Physiol*. 2020;235(6):5182–5191. doi:10.1002/jcp.29395
22. Yang TL, Guo Y, Li J, et al. Gene-gene interaction between RBMS3 and ZNF516 influences bone mineral density. *J Bone Miner Res*. 2013;28(4):828–837. doi:10.1002/jbmr.1788
23. Wang JJ, Liu XY, Du W, Liu JQ, Sun B, Zheng YP. RBMS3 delays disc degeneration by inhibiting Wnt/beta-catenin signaling pathway. *Eur Rev Med Pharmacol Sci*. 2020;24(2):499–507. doi:10.26355/eurrev_202001_20023
24. Werder R, Cho MH, Zhou AX, Kotton DN. Wilson AA: a CRISPRi approach to investigate GWAS genes in iPS-derived alveolar epithelial cells. *Am J Resp Crit Care*. 2021;203(9).
25. Nicoletti P, Cartsos VM, Palaska PK, Shen Y, Floratos A, Zavras AI. Genomewide pharmacogenetics of bisphosphonate-induced osteonecrosis of the jaw: the role of RBMS3. *Oncologist*. 2012;17(2):279–287. doi:10.1634/theoncologist.2011-0202
26. Majidinia M, Sadeghpour A, Yousefi B. The roles of signaling pathways in bone repair and regeneration. *J Cell Physiol*. 2018;233(4):2937–2948. doi:10.1002/jcp.26042
27. Lee HW, Suh JH, Kim HN, et al. Berberine promotes osteoblast differentiation by Runx2 activation with p38 MAPK. *J Bone Miner Res*. 2008;23(8):1227–1237. doi:10.1359/jbmr.080325
28. Ahmad M, Kruger BT, Kroll T, et al. Inhibition of Cdk5 increases osteoblast differentiation and bone mass and improves fracture healing. *Bone Res*. 2022;10(1):33. doi:10.1038/s41413-022-00195-z
29. Cappuzzo F, Ricciuti B, Delmonte A, et al. MAPK pathway-activating alteration and immunotherapy efficacy in squamous cell lung carcinoma: results from the randomized, prospective SQUINT trial. *Clin Cancer Res*. 2025;31(6):1027–1036. doi:10.1158/1078-0432.CCR-24-2077
30. Rozeman EA, Versluis JM, Sikorska K, et al. IMPemBra: a Phase 2 study comparing pembrolizumab with intermittent/short-term dual MAPK pathway inhibition plus pembrolizumab in patients with melanoma harboring the BRAFV600 mutation. *J Immunother Cancer*. 2023;11(7):e006821. doi:10.1136/jitc-2023-006821
31. Berger MD, Stintzing S, Heinemann V, et al. Impact of genetic variations in the MAPK signaling pathway on outcome in metastatic colorectal cancer patients treated with first-line FOLFIRI and bevacizumab: data from FIRE-3 and TRIBE trials. *Ann Oncol*. 2017;28(11):2780–2785. doi:10.1093/annonc/mdx412
32. Shin MH, Kim J, Lim SA, Kim J, Lee KM. Current insights into combination therapies with MAPK inhibitors and immune checkpoint blockade. *Int J Mol Sci*. 2020;21(7):2531. doi:10.3390/ijms21072531